Smart Structures Systems, *Vol. 20, No. 6 (2017) 709-728*
DOI: https://doi.org/10.12989/sss.2017.20.6.709

Nonlocal strain gradient-based vibration analysis of embedded curved porous piezoelectric nano-beams in thermal environment

Farzad Ebrahimi*, Mohsen Daman and Ali Jafari

Department of Mechanical Engineering, Faculty of Engineering, Imam Khomeini International University, Qazvin, Iran P.O.B. 16818-34149

(Received March 31, 2017, Revised August 25, 2017, Accepted September 15, 2017)

Abstract. This disquisition proposes a nonlocal strain gradient beam theory for thermo-mechanical dynamic characteristics of embedded smart shear deformable curved piezoelectric nanobeams made of porous electro-elastic functionally graded materials by using an analytical method. Electro-elastic properties of embedded curved porous FG nanobeam are assumed to be temperature-dependent and vary through the thickness direction of beam according to the power-law which is modified to approximate material properties for even distributions of porosities. It is perceived that during manufacturing of functionally graded materials (FGMs) porosities and micro-voids can be occurred inside the material. Since variation of pores along the thickness direction influences the mechanical and physical properties, so in this study thermo-mechanical vibration analysis of curve FG piezoelectric nanobeam by considering the effect of these imperfections is performed. Nonlocal strain gradient elasticity theory is utilized to consider the size effects in which the stress for not only the nonlocal stress field but also the strain gradients stress field. The governing equations and related boundary condition of embedded smart curved porous FG nanobeam subjected to thermal and electric field are derived via the energy method based on Timoshenko beam theory. An analytical Navier solution procedure is utilized to achieve the natural frequencies of porous FG curved piezoelectric nanobeam resting on Winkler and Pasternak foundation. The results for simpler states are confirmed with known data in the literature. The effects of various parameters such as nonlocality parameter, electric voltage, coefficient of porosity, elastic foundation parameters, thermal effect, gradient index, strain gradient, elastic opening angle and slenderness ratio on the natural frequency of embedded curved FG porous piezoelectric nanobeam are successfully discussed. It is concluded that these parameters play important roles on the dynamic behavior of porous FG curved nanobeam. Presented numerical results can serve as benchmarks for future analyses of curve FG nanobeam with porosity phases.

Keywords: curved piezoelectric FG nanobeam; porous materials; thermo-mechanical vibration; nonlocal strain gradient theory; smart materials; winkler-pasternak foundations

1. Introduction

Functionally graded materials (FGMs) are the new class of composites materials that provide wide spectrum of applications for various machineries which are under extreme thermo-mechanical loadings such as heat shields of spacecraft body, nuclear reactor components, jet fighter structures and heat engine components. Because of continuous variation of material properties in comparison with classical composites, FGMs have various advantages such as avoiding the cracking and delamination phenomenon, minimization or elimination of stress concentrations and residual stresses, ensuring smooth transition of stress distributions and so on. These new advanced materials were proposed by a group of Japanese scientists in the mid-1980s, as thermal barrier for aerospace applications (Koizumi and Niino 1995). The material properties of FGMs varies continuously in one or more directions. Due to high strength and high temperature resistance of FGMs, they are increasingly utilized as structural components in modern industries such as heat shields of spacecraft body, nuclear reactor components, jet fighter structures and heat engine components.(Mortensen and Suresh 2013).

The FGMs can be used to produce the shuttle structures. When the space shuttles enter to and from the atmosphere, due to friction between the vehicle surface and air with high velocity, the surface of the plane experiences temperature as high as 2100K. It is obvious that in this circumstance we need materials with super-heat-resistant properties to withstand high temperature and thermal impact in one side while on the other side (liquid hydrogen-cooled) we need materials with good toughness and thermal conductivity to ensure rapid cooling and a certain lifetime, hence it is essential to assume changing material properties due to thermal environment. FG structures resting on elastic foundations have wide applications in modern engineering.

The interaction of a structure with its foundation can be explained by suggesting various basic models in the literature. One of the simplest model for the elastic foundation is Winkler model because it takes the foundation into account as a set of independent and separate springs. Pasternak improved this model later by introducing a new

*Corresponding author, Professor
E-mail: febrahimy@gmail.com

ISSN: 1738-1584 (Print), 1738-1991 (Online)

dependence parameter that takes the interactions between the separated springs in Winkler model into account. In view of these advantages, a number of investigations, dealing with static, buckling, dynamic characteristics of FG structures, had been published in the scientific literature (Ebrahimi 2013, Ebrahimi *et al.* 2016a, Ebrahimi and Zia 2015, Ebrahimi and Mokhtari 2015). Ying *et al.* (2008) provided exact solution for bending and vibration embedded FG beam based on two dimensional elasticity theory. Thermo-mechanical vibration of FGM sandwich beam under variable elastic foundations by DQM analyzed by Pradhan and Murmu (2009). 3-D free vibration of thick functionally graded plates on elastic foundations was examined by Malekzadeh (2009). Benchmark solutions for FG thick plates resting on Winkler–Pasternak elastic foundations was introduced by Huang *et al.* (2008). DSC method was utilized for non-linear analysis of laminated plates resting on Winkler–Pasternak elastic foundations firstly by Civalek and Akgoz (2011). A 3-D free vibration of thick circular plates on Pasternak foundation was introduced by Zhou *et al.* (2006). Also, 3-D free vibration analysis of annular plates on Pasternak elastic foundation by p-Ritz method was examined by Hosseini Hashemi *et al.* (2008). For more efficient and expand applications of nano structures, they were recently synthesized by using FGMs. Actually, functionally graded model enables the nano materials to have the optimum properties.

Due to extensive applications of nano-structure made of FGM in advanced diverse technology, there has been intensive investigation about caption of nano materials with functional graded. The classical continuum theory is aptly practical in the mechanical behavior of the macroscopic structures, but it ignores the size-dependency of nano-structures, thereupon classical continuum theory is not suitable one to micro and nano scales structures. In order to bypass this drawback, two nonlocal elasticity theory namely Eringen's nonlocal elasticity theory (Eringen 2008, Eringen 1972a, b, Eringen 1983) and nonlocal strain gradient theory (Ying *et al.* 2008, Ebrahimi and Barati 2016) are offered to consider size effect. According to Eringen's model, the stress state at a certain point is considered as a function of strain states of all points in its area. Numerous studies have been conducted for investigation the mechanical responses of FG nano-beams and plates based on nonlocal elasticity theory (Ebrahimi and Salari 2015a, b, 2016, Ebrahimi *et al.* 2015a, 2016c, Ebrahimi and Nasirzadeh 2015, Ebrahimi and Barati 2016 a,b,c,d,e,f, Ebrahimi and Hosseini 2016 a,b,c). Based on nonlocal Timoshenko beam theory, Vibration characteristics of size dependent FG nanobeams is reported by Rahmani and Pedram (2014). Furthermore, Eltaher *et al.* (2012) presented free vibration analysis of functionally graded size-dependent nanobeams. Ebrahimi and Salari (2015c) provided differential transform method for flexural vibrational behavior of FG nanobeams. In another survey, Ebrahimi and Barati (2016) utilized a higher order refined beam theory for dynamic analysis of magneto electro embedded FG structures. Bounouara *et al.* (2016) provided zeroth-order shear deformation theory for free vibration analysis of embedded FG nanoplates. Notwithstanding the fact that nonlocal elasticity theory is widely utilized to consider the influence of small-scale, it considers only the stiffness softening influence. Many researchers have discovered increment in the stiffness of structures, which is disregarded in Eringen's nonlocal elasticity theory (Lam *et al.* 2003, Fleck and Hutchinson 1993, Stölken and Evans 1998). According to experimental research and as well as the strain gradient theory, the Eringen's nonlocal elasticity theory is unable to anticipate the influence of stiffness-hardening and strain gradient elasticity (Lam *et al.* 2003, Ebrahimi and Barati 2016) via introducing the length scale parameter. It is noted that, two exactly different physical Specifications were expressed by nonlocal theory and the strain gradient theory. Hereupon, nonlocal strain gradient theory is proposed to overcome the defect of nonlocal Eringen's theory with considering two length scales in a single theory (Lim *et al.* 2015). The two length scale parameters have an indeed influence on the physical and mechanical behavior of small size structures, which is considered in nonlocal strain gradient theory. By implementation of nonlocal strain gradient theory, buckling behavior of size-dependent nonlinear beams is presented by Li and Hu (2015). Based on size-dependent Timoshenko beam theory and employing the nonlocal strain gradient theory, Li *et al.* (2016) provided the Navier solution approach for vibration behavior of FG nanobeams. They reported that increasing in the nonlocal stress parameter causes the decrease in the non-dimensional frequency of FG nanobeams. However, for the length scale coefficient this behavior is vice versa. Furthermore, the flexural wave propagation response of Euler-Bernoulli FG beam was inspected by Li *et al.* (2015) within the framework of nonlocal strain gradient elasticity. Also, Ebrahimi and Barati (2017) examined hygro thermal impact on vibration behavior embedded FG nanobeams based on nonlocal strain gradient elasticity. Most recently Ebrahimi and Barati (2016g,h,i,j,k,l, 2017a,b) and Ebrahimi *et al.* (2017) explored thermal and hygro-thermal effects on nonlocal behavior of FG nanobeams and nanoplates.

Piezo electro materials as one of the special sorts of smart materials have received much attention in engineering structures during the recent years. In 1990s, a strong electrical coupling effect was discovered which has potential practical application in many fields (Harshe *et al.* 1993, Nan 1994, Benveniste 1995) and reported that this coupling effect cannot be found in a single-phase material. Furthermore, piezo electro materials show fascinating properties, influences in which the elastic deformations may be produced directly by mechanical loading or indirectly by an application of electric field. The mechanical behaviors of electro-elastic structures have received notable attention by many researchers in the recent years.

Structures made of porous materials are the latest developments in the field of FGMs, so it is vital to consider influence of porosity parameters in their dynamic analysis (Ebrahimi and Jafari 2016 a, b, c). The presence of pores within the microstructures of such materials are taken into account by means of the local density of the material. Typically, common composition of FGMs is ceramic-metal and there are different approaches for processing of functionally graded metal–ceramic composite components

(Ebrahimi and Jafari 2017). In some process of fabrication for producing the FGMs, porosities and micro-voids can be occurring inside the materials due to technical problems. For instance, different shrinkage stresses between the adjacent layers of ceramic and metal phases in FGM compact can be occurs during the processes of sintering and cold compacting, which may create porosity phases inside the materials (Ebrahimi *et al.* 2016). Moreover, in the multi-step sequential infiltration method for producing FGMs, it is observed that the most of the porosity phases appear frequently in the central areas of FGM specimens because it is hard to infiltrate the secondary material in these zones completely, whereas material infiltration at the bottom and top areas can be performed easier with less porosities. According to this information, it is necessary to consider the influences of these imperfections on vibration behavior of FGMs structures carrying porosities (Ebrahimi *et al.* 2017).

There are a lot of studies related to dynamic and stability behaviors of FG structures but the dynamic analysis of porous FG structures, especially for beams, are still limited in number. For porous plates, the wave propagation of FG plates having porosities by using various higher-order shear deformation theories has been studied by Ait Yahia *et al.* (2015). Recently, Mechab *et al.* (2016) developed a nonlocal elasticity model for free vibration of FG porous nanoplates resting on elastic foundations. Wattanasakulpong and Ungbhakorn (2014) investigated linear and non-linear vibration of porous FGM beams with elastically restrained ends. In another work, Wattanasakulpong and Chaikittiratana (2015) predicted flexural vibration of porous FGM beams by applying the Chebyshev collocation method (CCM). Ebrahimi and Zia (2015) investigated the large-amplitude nonlinear vibration of porous FGM beams by utilizing Galerkin and multiple scales methods. Boutahar *et al.* (2016) presented a semi analytical method for non-linear vibration analysis of FGM porous annular plates resting on elastic foundations.

Huge application of curve nanobeams and nanoring in the empirical experiments and dynamic molecular simulations (Wang and Duan 2008) led many researchers to study the mechanical characteristics of these structures. In comparison with straight nanobeams, curved ones possess various advantages such as large strokes (Ebrahimi and Barati 2016). Recently, the use of curved nanobeams has been extended in different systems as nanoswitches, nanovalves and nanofilters. Literature survey indicates that there are few researches about vibration behavior of FGM curved nanostructures like beam, ring and arches. Yan and Jiang (2011) investigated the electromechanical response of curved piezoelectric nanobeam with the consideration of surface effects. In addition, a new numerical technique, the differential quadrature method has been developed for dynamic analysis of the nanobeams in the polar coordinate system by Kananipour *et al.* (2014). In addition, investigating surface effects on thermomechanical behavior of embedded circular curved nanosize beams has been studied by Ebrahimi and Daman (2016). However, Ebrahimi and Daman (2016) have presented the radial vibration of embedded double-curved-nanobeam-systems. As well as, Wang and Duan (2008) have surveyed the free vibration problem of nanorings/arches. In this research the problem was formulated framework of Eringen's nonlocal theory of elasticity according to allow for the small length scale effect. Also, dynamic modeling of embedded curved nanobeams incorporating surface effects has been presented by Ebrahimi and Daman (2016). In addition, Ebrahimi and Daman (2017) have studied analytical investigation of the surface effects on nonlocal vibration behavior of nanosize curved beams. Moreover, Ansari *et al.* (2013), developed vibration of FG curved microbeams with Out-of-plane frequency analyze of FG circular curved beams in thermal environment has been investigated by Malekzadeh *et al.* (2010). In addition, Hosseini and Rahmani (2016) presented free vibration of shallow and deep curved functionally graded nanobeam based on nonlocal Timoshenko curved beam model. Moreover, Ebrahimi and Barati (2017) employed nonlocal strain gradient theory to model size-dependent buckling response of FG curve nanobeams with different boundary conditions.

Reviewing the literature search in the field of vibration behavior of FG curve nanobeam indicates that there is not any published work considering small size effects, strain gradient, porosity, thermal effect, elastic foundation and electric voltage on vibration characteristics of FG curve nanobeam based on Timoshenko beam theory. As a result, present research analyzes thermo-mechanical vibration of curved FG porous embedded nanobeams exposed to electric voltage based on nonlocal strain gradient theory which consider both nonlocal and length scale parameter to describe size effects. Curvature rather exists in all of the real beams and nanobeams. Moreover, in previous researches in order to streamline of mathematical equations, straight beam models have been used, whilst curved beam models are more practicable than straight ones. The modified power-law model is exploited to describe gradual variation of thermo-mechanical properties of the porous FG piezo curve nanobeam. Applying Hamilton's principle, governing equations of porous FG curve nanobeam are obtained together and they are solved applying an analytical solution method. Dimensionless natural frequencies are obtained respect to the effect of various parameters such as angle of curvature, length scale parameter, temperatures changes, Winkler-Pasternak foundation parameters, mode numbers, power-law index, electric voltage and nonlocal parameter on vibration of curved porous FG piezo nanobeams. Comparison between the results of present research and available data in literature reveals the accuracy of this model.

2. Problem formulation

2.1 The material properties of curved FGP nanobeams

A curved FGP nanobeam made of piezoelectric materials involved PZT-4 and PZT-5H with length L in θ direction and uniform thickness h in z direction, and under an electric potential $\varphi(\theta,z,t)$ as shown in Fig. 1 is assumed.

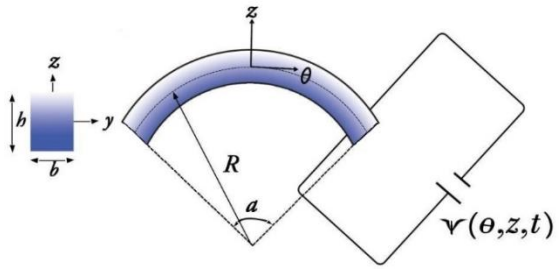

Fig. 1 Geometric of curved FGP nanobeam

The relation between length of circular curved beam (θ) and the angle of curvature of beam (α) can be written as (Setoodeh *et al*. 2015).

$$\theta = R\alpha \tag{1}$$

The effective material properties of the curved FGPM beam are assumed to vary continuously in the thickness direction based on a power-law model. According to this model, the effective material properties, *P*, can be defined as follow (Komijani *et al.* 2014).

$$P = P_u V_u + P_l V_l \tag{2}$$

where (P_l, P_u) are the properties of materials at the lower surface and upper surface, respectively. In addition, (V_l, V_u) are the corresponding volume fractions related by (Wattanasakulpong *et al.* 2011)

$$V_u = \left(\frac{z}{h} + \frac{1}{2}\right)^p \tag{3}$$

$$V_u + V_l = 1 \tag{4}$$

Hence, from Eqs. (2) and (3), the impressive material properties of the curved FGP beam can be defined as (Fallah and Aghdam 2011)

$$P(z) = (P_u - P_l)\left(\frac{z}{h} + \frac{1}{2}\right)^p + P_l \tag{5}$$

where *p* is the nonnegative variable parameter (power-law exponent). Power-law exponent determines the distribution profile of material through the thickness of the beam in *z* direction. Based on this distribution, the bottom surface is pure PZT-5H, whiles the top surface of curved FGP nanobeam stands for pure PZT-4.

2.2 Governing equation

Based on Timoshenko beam theory, displacement field in a point of the curved beam model can be remarked as

$$u_\theta(\theta, z, t) = \left(1 + \frac{z}{R}\right)u(\theta, t) + z\varphi(\theta, t) \tag{6a}$$

$$u_z(\theta, z, t) = w(\theta, t) \tag{6b}$$

where *w* and *u* interpret the radial and tangential displacement of curved FGP beam. In addition, φ is total bending rotation of cross sections of curved FGP beam. The strains of Timoshenko curved beam theory may be expressed as

$$\varepsilon^0_{\theta\theta} = \frac{\partial w}{\partial \theta} - \frac{u}{R} \tag{7b}$$

$$\kappa = \frac{\partial \varphi}{\partial \theta} \tag{7b}$$

$$\gamma_{\theta z} = \frac{\partial u}{\partial \theta} - \varphi + \frac{w}{R} \tag{7c}$$

Here γ denotes shear strain in curved beam model.

$$E_\theta = -\frac{\partial \psi}{\partial \theta} = Cos(\beta z)\frac{\partial \psi}{\partial \theta} \tag{8b}$$

$$E_z = -\frac{\partial \psi}{\partial z} = -\beta Sin(\beta z)\psi - \frac{2V_0}{h}e^{i\Omega t} \tag{8b}$$

$$\varepsilon_{\theta\theta} = \left(\varepsilon^0_{\theta\theta} + z\kappa\right) \tag{9}$$

The energy method (Hamilton's principle) can be employed to derive the governing equations as follow

$$\int_0^t \delta(U_s - T + W_{ext}) = 0 \tag{10}$$

where U_s, T and W_{ext} are strain energy, kinetic energy and work done by external exerted loads, respectively. The first variation of strain energy U_s can be determined as

$$\delta U_s = \int_V \left(\sigma_{\theta\theta}\delta\varepsilon_{\theta\theta} + \sigma_{\theta z}\delta\gamma_{\theta z} - D_\theta \delta E_\theta - D_z \delta E_z\right)dV \tag{11}$$

By inserting Eqs. (6) and (7) in Eq. (10), first variation of strain energy can be obtained as

$$\begin{aligned}\delta U_s = &\int_0^L \left(N\left(-\frac{\delta u}{R} + \frac{\partial \delta w}{\partial \theta}\right) + M\left(\frac{\partial \delta \varphi}{\partial \theta}\right) + Q\left(\frac{\partial \delta u}{\partial \theta} - \delta\varphi + \frac{\delta w}{R}\right)\right)d\theta \\ &+ \int_0^L \int_{\frac{-h}{2}}^{\frac{h}{2}} \left(D_z \beta Sin(\beta z)\delta\psi - D_\theta Cos(\beta z)\frac{\partial \delta \psi}{\partial \theta}\right)dz d\theta\end{aligned} \tag{12}$$

Here *M*, *N*, and *Q* define bending moment of cross section, axial force, and shear force, respectively. These stress resultants existing in Eq. (12) may be expressed as

$$N = \int_A \sigma_{\theta\theta} dA \tag{13}$$

$$M = \int_A \sigma_{\theta\theta} z dA$$
$$Q = \int_A K_{shear} \sigma_{\theta z} dA$$

where K_{Shear} expresses the shear correction factor. In addition, Kinetic energy of Timoshenko curved beam can be calculated as

$$T = \frac{1}{2}\int_0^L \int_A \rho(z)\left(\left(\frac{\partial u_\theta}{\partial t}\right)^2 + \left(\frac{\partial u_z}{\partial \theta}\right)^2\right) dA d\theta \tag{14}$$

Hence, first variation of kinetic energy can be calculated as

$$\delta T = \begin{bmatrix} I_0\left(\frac{\partial u}{\partial t}\frac{\partial \delta u}{\partial t}\right) + \left(I_0 + \frac{2I_1}{R} + \frac{I_2}{R^2}\right)\frac{\partial w}{\partial t}\frac{\partial \delta w}{\partial t} \\ + \left(I_1 + \frac{I_2}{R}\right)\left(\frac{\partial \varphi}{\partial t}\frac{\partial \delta w}{\partial t} + \frac{\partial w}{\partial t}\frac{\partial \delta \varphi}{\partial t}\right) + I_2 \frac{\partial \varphi}{\partial t}\frac{\partial \delta \varphi}{\partial t} \end{bmatrix} d\theta \tag{15}$$

where mass moments of inertias (I_0, I_1, I_2) are calculated as follows

$$(I_0, I_1, I_2) = \int_A \rho(z)(1, z, z^2) dA \tag{16}$$

Whereas the work done by the external loads is defined by W_{ext}

$$\delta W_{ext} = \frac{1}{2}\int_0^L (N_E + N_T)\frac{\partial w}{\partial \theta}\delta\frac{\partial w}{\partial \theta} + \left(-K_W \delta w + K_P \frac{\partial^2 \delta w}{\partial \theta^2}\right) d\theta \tag{17}$$

where N_E and N_T are the external electric voltage V_0 and temperature changes ΔT, which can be given as

$$N_T = \int_{\frac{-h}{2}}^{\frac{h}{2}} c_{11}\lambda_1 \Delta T dz$$
$$N_E = -\int_{\frac{-h}{2}}^{\frac{h}{2}} 2e_{31}\frac{V_0}{h} dz \tag{18}$$

By inserting δu, δw, $\delta\varphi$ and $\delta\psi$ coefficients equal to zero, following equation of motions can be determined for curved FGP nanobeam

$$\frac{N}{R} + \frac{\partial Q}{\partial \theta} = I_0 \frac{\partial^2 u}{\partial t^2} \tag{19a}$$

$$\frac{\partial N}{\partial \theta} - \frac{Q}{R} - (N_T + N_E)\frac{\partial^2 w}{\partial \theta^2} = \left(I_0 + \frac{2I_1}{R} + \frac{I_2}{R^2}\right)\frac{\partial^2 w}{\partial t^2} + \left(I_1 + \frac{I_2}{R}\right)\frac{\partial^2 \varphi}{\partial t^2} + K_W w - K_P \frac{\partial^2 w}{\partial \theta^2} \tag{19b}$$

$$\frac{\partial M}{\partial \theta} + Q = \left(I_1 + \frac{I_2}{R}\right)\frac{\partial^2 w}{\partial t^2} + I_2 \frac{\partial^2 \varphi}{\partial t^2} \tag{19c}$$

$$\int_{\frac{-h}{2}}^{\frac{h}{2}} \frac{\partial D_\theta}{\partial \theta} Cos(\beta z) dz + \int_{\frac{-h}{2}}^{\frac{h}{2}} D_z \beta Sin(\beta z) dz = 0 \tag{19d}$$

Boundary conditions that are related to equation of motions are considered as

$$N = 0 \text{ or } w = 0 \text{ at } \theta = 0 \text{ and } \theta = L \tag{20a}$$

$$Q = 0 \text{ or } u = 0 \text{ at } \theta = 0 \text{ and } \theta = L \tag{20a}$$

$$M = 0 \text{ or } \varphi = 0 \text{ at } \theta = 0 \text{ and } \theta = L \tag{20c}$$

$$\int_{\frac{-h}{2}}^{\frac{h}{2}} D_\theta Cos(\beta z) dz = 0 \text{ or } \psi = 0 \text{ at } \theta = 0 \text{ and } \theta = L \tag{20d}$$

2.3 *The nonlocal elasticity model for curved FG nanobeam*

Despite the fundamental equations in classic elasticity theory, Eringen's nonlocal model explains that the stress at a certain point *x* in a body is assumed as a function of strains of all points x' in the near realm. This supposition is very good agreement with experiments of atomic model and lattice dynamics in phonon scattering in which for a nonlocal piezoelectric materials. The basic equations with zero body force can be given as (Ke *et al*. 2012).

$$\sigma_{ij} = \int_V \alpha(|x' - x|, \tau)\begin{bmatrix} C_{ijkl}\varepsilon_{kl}(x') - e_{kij}E_k(x') \\ -C_{ijkl}\alpha_{kl}\Delta T \end{bmatrix} dV(x') \tag{21a}$$

$$D_i = \int_V \alpha(|x' - x|, \tau)\begin{bmatrix} e_{ikl}\varepsilon_{kl}(x') \\ +k_{ik}E_k(x') + p_i\Delta T \end{bmatrix} dV(x') \tag{21b}$$

where σ_{ij}, ε_{ij}, D_i and E_i are the stress, strain, electric displacement and electric field components, respectively; ΔT and α_{kl} are the temperature changes and thermal expansion coefficient, respectively; C_{ijkl}, e_{kij}, k_{ik} and p_i are elastic, piezoelectric, dielectric and pyroelectric constants, respectively; $\alpha(|x' - x|, \tau)$ is the nonlocal kernel function and $|x' - x|$ is the nonnegative distance. $\tau = e_0 a / l$ is given as size coefficient.

The relations in Eq. (21) causes the elasticity problems difficult to solve, in addition to possible lack of

determinism. Eringen (2002) presented in detail properties of non-local kernel $\alpha\left(|x'-x|\right)$ and evaluated that when a kernel takes a Green's function of linear differential operator

$$L\alpha\left(|x'-x|\right)=\delta\left(|x'-x|\right) \tag{22}$$

By matching the scattering curves with lattice models, Eringen (2002) supposed a nonlocal theory with the linear differential operator *L* expressed as follow

$$L=1-\left(e_0 a\right)^2\nabla^2 \tag{23}$$

where ∇^2 is the Laplacian operator. Therefore, the fundamental relations given by Eq. (21) for nonlocal elasticity may be rewritten by differentiable form as

$$\begin{aligned}&\sigma_{ij}-\left(e_0 a\right)^2\nabla^2\sigma_{ij}=C_{ijkl}\varepsilon_{kl}\\&-e_{kij}E_k-C_{ijkl}\alpha_{kl}\Delta T\end{aligned} \tag{24a}$$

$$\begin{aligned}&D_i-\left(e_0 a\right)^2\nabla^2 D_i=e_{ikl}\varepsilon_{kl}\\&+k_{ik}E_k+p_i\Delta T\end{aligned} \tag{24b}$$

The parameter $e_0 a$ is the scale coefficient disclosing the nano scale effect on the responses of structures of nanoscale. The nonlocal parameter, $\mu=\left(e_0 a\right)$ is experimentally determined for different materials.

For a curved FGPM nanobeam under thermo-electro-mechanical loading in the one dimensional case, the nonlocal fundamental relations (24(a)) and (24(b)) can be streamlined as

$$\sigma_{\theta\theta}-\mu^2\frac{\partial^2\sigma_{\theta\theta}}{\partial\theta^2}=c_{11}\varepsilon_{\theta\theta}-e_{31}E_z-c_{11}\lambda_1\Delta T \tag{25a}$$

$$\sigma_{\theta z}-\mu^2\frac{\partial^2\sigma_{\theta z}}{\partial\theta^2}=c_{55}\gamma_{\theta z}-e_{15}E_\theta \tag{25b}$$

$$D_\theta-\mu^2\frac{\partial^2 D_\theta}{\partial\theta^2}=e_{15}\gamma_{\theta z}+k_{11}E_\theta \tag{25c}$$

$$D_z-\mu^2\frac{\partial^2 D_z}{\partial\theta^2}=e_{31}\varepsilon_{\theta\theta}+k_{33}E_z+p_3\Delta T \tag{25d}$$

Calculating Eqs. (25) by integrating over cross-section area of the curved beam, force–strain and moment–strain of nonlocal curved FGP Timoshenko beam model will be determined as

$$\begin{aligned}&N-\mu^2\frac{\partial^2 N}{\partial\theta^2}=A\left(\frac{\partial w}{\partial\theta}-\frac{u}{R}\right)\\&+B\frac{\partial\varphi}{\partial\theta}+B_{31}\psi\end{aligned} \tag{26a}$$

$$\begin{aligned}&M-\mu^2\frac{\partial^2 M}{\partial\theta^2}=B\left(\frac{\partial w}{\partial\theta}-\frac{u}{R}\right)\\&+D\frac{\partial\varphi}{\partial\theta}+F_{31}\psi\end{aligned} \tag{26b}$$

$$\begin{aligned}&Q-\mu^2\frac{\partial^2 Q}{\partial\theta^2}=K_{Shear}C\left(\frac{w}{R}+\frac{\partial u}{\partial\theta}-\varphi\right)\\&-K_{Shear}E_{15}\frac{\partial\psi}{\partial\theta}\end{aligned} \tag{26c}$$

$$\begin{aligned}&\int_{\frac{-h}{2}}^{\frac{h}{2}}\left[D_\theta-\mu^2\frac{\partial^2 D_\theta}{\partial\theta^2}\right]Cos\left(\beta z\right)dz\\&=K_{Shear}E_{15}\left(\frac{w}{R}+\frac{\partial u}{\partial\theta}-\varphi\right)+X_{11}\frac{\partial\psi}{\partial\theta}\end{aligned} \tag{26d}$$

$$\begin{aligned}&\int_{\frac{-h}{2}}^{\frac{h}{2}}\left[D_z-\mu^2\frac{\partial^2 D_z}{\partial\theta^2}\right]\beta Sin\left(\beta z\right)dz\\&=B_{31}\left(\frac{\partial w}{\partial\theta}-\frac{u}{R}\right)+F_{31}\frac{\partial\varphi}{\partial\theta}-X_{33}\psi\end{aligned} \tag{26e}$$

where K_{Shear} defined as correction factor and assumed that equal $5/6$. Consequently, coefficients are obtained as

$$\left\{A,B,D\right\}=\int_A c_{11}\left\{1,z,z^2\right\}dA \tag{27a}$$

$$C=\int_A c_{55}dA \tag{27b}$$

$$\left\{B_{31},F_{31},E_{15}\right\}=\int_A\begin{Bmatrix}e_{31}\beta Sin\left(\beta z\right),ze_{31}\beta Sin\left(\beta z\right)\\,e_{15}Cos\left(\beta z\right)\end{Bmatrix}dA \tag{27c}$$

$$\left\{X_{11},X_{33}\right\}=\int_A\begin{Bmatrix}\varepsilon_{11}Cos^2\left(\beta z\right)\\,\varepsilon_{33}\beta^2 Sin^2\left(\beta z\right)\end{Bmatrix}dA \tag{27d}$$

By inserting Eqs. (27) into Eqs. (19), nonlocal governing equations of curved FGP Timoshenko nanobeam in terms of displacement can be calculated as

$$\begin{aligned}&A\left(\frac{\partial w}{\partial\theta}-\frac{u}{R}\right)-A\lambda\left(\frac{\partial^3 w}{\partial\theta^3}-\frac{\partial^2 u}{R\partial\theta^2}\right)+\\&B\frac{\partial\varphi}{\partial\theta}-B\lambda\frac{\partial^3\varphi}{\partial\theta^3}+B_{31}\psi-B_{31}\lambda\frac{\partial^2\psi}{\partial\theta^2}+\\&K_{Shear}CR\left(\frac{\partial w}{R\partial\theta}+\frac{\partial^2 u}{\partial\theta^2}-\frac{\partial\varphi}{\partial\theta}\right)\\&-K_{Shear}CR\lambda\left(\frac{\partial^3 w}{R\partial\theta^3}+\frac{\partial^4 u}{\partial\theta^4}-\frac{\partial^3\varphi}{\partial\theta^3}\right)-K_{Shear}E_{15}R\frac{\partial^2\psi}{\partial\theta^2}\\&+K_{Shear}E_{15}R\lambda\frac{\partial^4\psi}{\partial\theta^4}=RI_0\left(\frac{\partial^2 u}{\partial t^2}-\mu^2\frac{\partial^4 u}{\partial\theta^2\partial t^2}\right)\end{aligned} \tag{28a}$$

$$
\begin{aligned}
&AR\left(\frac{\partial^2 w}{\partial\theta^2}-\frac{\partial u}{R\partial\theta}\right)-AR\lambda\left(\frac{\partial^4 w}{\partial\theta^4}-\frac{\partial^3 u}{R\partial\theta^3}\right)+\\
&BR\frac{\partial^2\varphi}{\partial\theta^2}-BR\lambda\frac{\partial^4\varphi}{\partial\theta^4}+B_{31}R\frac{\partial\psi}{\partial\theta}-B_{31}R\lambda\frac{\partial^3\psi}{\partial\theta^3}-\\
&\left(N_T+N_E\right)R\frac{\partial^2 w}{\partial\theta^2}+\mu^2\left(N_T+N_E\right)R\frac{\partial^4 w}{\partial\theta^4}-K_{Shear}C\\
&\left(\frac{w}{R}+\frac{\partial u}{\partial\theta}-\varphi\right)+K_{Shear}C\lambda\left(\frac{\partial^2 w}{R\partial\theta^2}+\frac{\partial^3 u}{\partial\theta^3}-\frac{\partial^2\varphi}{\partial\theta^2}\right)+\\
&K_{Shear}E_{15}\frac{\partial\psi}{\partial\theta}-K_{Shear}E_{15}\lambda\frac{\partial^3\psi}{\partial\theta^3}-K_W w+K_P\frac{\partial^2 w}{\partial\theta^2}-\\
&\mu^2\left(-K_W\frac{\partial^2 w}{\partial\theta^2}+K_P\frac{\partial^4 w}{\partial\theta^4}\right)=\left(I_0+\frac{2I_1}{R}+\frac{I_2}{R^2}\right)R\frac{\partial^2 w}{\partial t^2}\\
&+\left(I_1+\frac{I_2}{R}\right)R\frac{\partial^2\varphi}{\partial t^2}-\mu^2\left(I_0+\frac{2I_1}{R}+\frac{I_2}{R^2}\right)R\frac{\partial^4 w}{\partial\theta^2\partial t^2}-\\
&\mu^2\left(I_1+\frac{I_2}{R}\right)R\frac{\partial^4\varphi}{\partial\theta^2\partial t^2}
\end{aligned}
\tag{28b}
$$

$$
\begin{aligned}
&B\left(\frac{\partial^2 w}{\partial\theta^2}-\frac{\partial u}{R\partial\theta}\right)-B\lambda\left(\frac{\partial^4 w}{\partial\theta^4}-\frac{\partial^3 u}{R\partial\theta^3}\right)\\
&+D\frac{\partial^2\varphi}{\partial\theta^2}-D\lambda\frac{\partial^4\varphi}{\partial\theta^4}+F_{31}\frac{\partial\psi}{\partial\theta}-F_{31}\lambda\frac{\partial^3\psi}{\partial\theta^3}+\\
&K_{Shear}C\left(\frac{w}{R}+\frac{\partial u}{\partial\theta}-\varphi\right)-K_{Shear}C\lambda\left(\frac{\partial^2 w}{R\partial\theta^2}+\frac{\partial^3 u}{\partial\theta^3}-\frac{\partial^2\varphi}{\partial\theta^2}\right)-\\
&K_{Shear}E_{15}\frac{\partial\psi}{\partial\theta}+K_{Shear}E_{15}\lambda\frac{\partial^3\psi}{\partial\theta^3}=\left(I_1+\frac{I_2}{R}\right)\frac{\partial^2 w}{\partial t^2}+I_2\frac{\partial^2\varphi}{\partial t^2}-\\
&\mu^2\left(I_1+\frac{I_2}{R}\right)\frac{\partial^4 w}{\partial\theta^2\partial t^2}-\mu^2 I_2\frac{\partial^4\varphi}{\partial\theta^2\partial t^2}
\end{aligned}
\tag{28c}
$$

$$
\begin{aligned}
&E_{15}\left(\frac{\partial w}{R\partial\theta}+\frac{\partial^2 u}{\partial\theta^2}-\frac{\partial\varphi}{\partial\theta}\right)-E_{15}\lambda\left(\frac{\partial^3 w}{R\partial\theta^3}+\frac{\partial^4 u}{\partial\theta^4}-\frac{\partial^3\varphi}{\partial\theta^3}\right)\\
&+X_{11}\frac{\partial^2\psi}{\partial\theta^2}-X_{11}\lambda\frac{\partial^4\psi}{\partial\theta^4}+B_{31}\left(\frac{\partial w}{\partial\theta}-\frac{u}{R}\right)-B_{31}\lambda\left(\frac{\partial^3 w}{\partial\theta^3}-\frac{\partial^2 u}{R\partial\theta^2}\right)\\
&+F_{31}\frac{\partial\varphi}{\partial\theta}-F_{31}\lambda\frac{\partial^3\varphi}{\partial\theta^3}-X_{33}\psi+X_{33}\lambda\frac{\partial^2\psi}{\partial\theta^2}=0
\end{aligned}
\tag{28d}
$$

3. Solution method

In this section, analytical Navier method has been developed to solve the governing equations of curved FGP in regard to find out free vibrational of a simply supported curved FGP nanobeam. However, to define the displacement functions, product of unknown factors and known trigonometric functions has been employed to satisfy the governing equations and boundary conditions at $\theta=0,\ L$ ends. The displacement fields are assumed to be as follows

$$w(\theta,t)=\sum_{n=1}^{\infty}W_n Cos\left(\frac{n\pi}{L}\theta\right)e^{i\omega_n t} \tag{29a}$$

$$u(\theta,t)=\sum_{n=1}^{\infty}U_n Sin\left(\frac{n\pi}{L}\theta\right)e^{i\omega_n t} \tag{29b}$$

$$\varphi(\theta,t)=\sum_{n=1}^{\infty}\phi_n Cos\left(\frac{n\pi}{L}\theta\right)e^{i\omega_n t} \tag{29c}$$

$$\psi(\theta,t)=\sum_{n=1}^{\infty}\psi_n Sin\left(\frac{n\pi}{L}\theta\right)e^{i\omega_n t} \tag{29d}$$

where W_n, U_n, ϕ_n and ψ_n are the unknown Fourier factors to be obtained for each *n* value. The boundary conditions for simply supported curved FGP nanobeam can be given as

$$
\begin{aligned}
&w(0)=0,\ \frac{\partial w}{\partial\theta}(L)=0,\ u(0)=u(L)=0\\
&\frac{\partial\varphi}{\partial\theta}(0)=\frac{\partial\varphi}{\partial\theta}(L)=0,\ \psi(0)=\psi(L)=0
\end{aligned}
\tag{30}
$$

Inserting Eqs. (29) into Eqs. (28) respectively, leads to Eqs. (30)

$$
\begin{aligned}
&A\left(-\frac{U_n}{R}-\left(\frac{n\pi}{L}\right)W_n\right)+A\lambda\left(\frac{n\pi}{L}\right)^2\left(-\frac{U_n}{R}-\left(\frac{n\pi}{L}\right)W_n\right)\\
&-B\left(\frac{n\pi}{L}\right)\phi_n-B\lambda\left(\frac{n\pi}{L}\right)^3\phi+B_{31}\psi_n+B_{31}\lambda\left(\frac{n\pi}{L}\right)^2\psi_n\\
&+K_{Shear}CR\left[-\frac{1}{R}\left(\frac{n\pi}{L}\right)W_n-\left(\frac{n\pi}{L}\right)^2U_n+\left(\frac{n\pi}{L}\right)\phi_n\right]+\\
&K_{Shear}CR\lambda\left(\frac{n\pi}{L}\right)^2\left[-\frac{1}{R}\left(\frac{n\pi}{L}\right)W_n-\left(\frac{n\pi}{L}\right)^2U_n+\left(\frac{n\pi}{L}\right)\phi_n\right]+\\
&K_{Shear}E_{15}R\left(\frac{n\pi}{L}\right)^2\psi_n+K_{Shear}E_{15}R\lambda\left(\frac{n\pi}{L}\right)^4\psi_n=\\
&RI_0\left(-\omega_n^2U_n-\mu^2\omega_n^2\left(\frac{n\pi}{L}\right)^2U_n\right)
\end{aligned}
\tag{31a}
$$

$$
\begin{aligned}
&AR\left[-\frac{1}{R}\left(\frac{n\pi}{L}\right)U_n-\left(\frac{n\pi}{L}\right)^2W_n\right]+AR\lambda\left(\frac{n\pi}{L}\right)^2\\
&\left[-\frac{1}{R}\left(\frac{n\pi}{L}\right)U_n-\left(\frac{n\pi}{L}\right)^2W_n\right]-BR\left(\frac{n\pi}{L}\right)^2\phi_n-\\
&BR\lambda\left(\frac{n\pi}{L}\right)^4\phi_n+B_{31}R\left(\frac{n\pi}{L}\right)\psi_n+B_{31}R\lambda\left(\frac{n\pi}{L}\right)^3\psi_n\\
&-\left(N_T+N_E\right)R\left(\frac{n\pi}{L}\right)^2W_n-\mu^2\left(N_T+N_E\right)R\left(\frac{n\pi}{L}\right)^4W_n\\
&-K_{Shear}C\left[\frac{1}{R}W_n+\left(\frac{n\pi}{L}\right)U_n-\phi_n\right]-K_{Shear}C\lambda\left(\frac{n\pi}{L}\right)^2\\
&\left[\frac{1}{R}W_n+\left(\frac{n\pi}{L}\right)U_n-\phi_n\right]+K_{Shear}E_{15}\left(\frac{n\pi}{L}\right)\psi_n+\\
&K_{Shear}E_{15}\lambda\left(\frac{n\pi}{L}\right)^3\psi-K_WW_n-K_P\left(\frac{n\pi}{L}\right)^2W_n\\
&-\mu^2\left(-K_W\left(\frac{n\pi}{L}\right)^2W_n-K_P\left(\frac{n\pi}{L}\right)^4W_n\right)+=\\
&-\left(I_0+\frac{2I_1}{R}+\frac{I_2}{R^2}\right)R\omega_n^2W_n-\left(I_1+\frac{I_2}{R}\right)R\omega_n^2\phi_n-\\
&\mu^2R\left(\frac{n\pi}{L}\right)^2\left(I_0+\frac{2I_1}{R}+\frac{I_2}{R^2}\right)\omega_n^2W_n-\mu^2\left(I_1+\frac{I_2}{R}\right)R\left(\frac{n\pi}{L}\right)^2\omega_n^2\phi_n
\end{aligned}
\tag{31b}
$$

$$
\begin{aligned}
&BR\left[-\frac{1}{R}\left(\frac{n\pi}{L}\right)U_n+\left(\frac{n\pi}{L}\right)^2W_n\right]+BR\lambda\left(\frac{n\pi}{L}\right)^2\\
&\left[-\frac{1}{R}\left(\frac{n\pi}{L}\right)U_n+\left(\frac{n\pi}{L}\right)^2W_n\right]-RD\left(\frac{n\pi}{L}\right)^2-\\
&RD\lambda\left(\frac{n\pi}{L}\right)^4\phi_n+F_{31}R\left(\frac{n\pi}{L}\right)\psi_n+F_{31}R\lambda\left(\frac{n\pi}{L}\right)^3\psi\\
&+K_{Shear}CR\left[\frac{1}{R}W_n+\left(\frac{n\pi}{L}\right)U_n-\phi_n\right]+K_{Shear}CR\lambda \qquad (31c)\\
&\left(\frac{n\pi}{L}\right)^2\left[\frac{1}{R}W_n+\left(\frac{n\pi}{L}\right)U_n-\phi_n\right]-K_{Shear}E_{15}R\\
&\left(\frac{n\pi}{L}\right)\psi_n-K_{Shear}E_{15}R\lambda\left(\frac{n\pi}{L}\right)^3\psi_n=-R\left(I_1+\frac{I_2}{R}\right)\omega_n^2W_n\\
&-RI_2\omega_n^2\phi_n-R\mu^2\left(I_1+\frac{I_2}{R}\right)\left(\frac{n\pi}{L}\right)^2\omega_n^2W_n--R\mu^2I_2\left(\frac{n\pi}{L}\right)^2\omega_n^2\phi_n
\end{aligned}
$$

$$
\begin{aligned}
&-K_{Shear}E_{15}R\left[-\frac{1}{R}\left(\frac{n\pi}{L}\right)W_n-\left(\frac{n\pi}{L}\right)^2U_n+\left(\frac{n\pi}{L}\right)\phi_n\right]\\
&-K_{Shear}E_{15}R\lambda\left(\frac{n\pi}{L}\right)^2\\
&\left[-\frac{1}{R}\left(\frac{n\pi}{L}\right)W_n-\left(\frac{n\pi}{L}\right)^2U_n+\left(\frac{n\pi}{L}\right)\phi_n\right]\\
&+X_{11}R\left(\frac{n\pi}{L}\right)^2\psi_n+X_{11}R\lambda\left(\frac{n\pi}{L}\right)^4\psi_n- \qquad (31d)\\
&RB_{31}\left[-\frac{1}{R}U_n-\left(\frac{n\pi}{L}\right)W_n\right]-RB_{31}\lambda\left(\frac{n\pi}{L}\right)^2\\
&\left[-\frac{1}{R}U_n-\left(\frac{n\pi}{L}\right)W_n\right]+RF_{31}\left(\frac{n\pi}{L}\right)\phi\\
&{}_n+RF_{31}\lambda\left(\frac{n\pi}{L}\right)^3\phi+RX_{33}\psi_n+RX_{33}\lambda\left(\frac{n\pi}{L}\right)^2\psi_n
\end{aligned}
$$

By inserting the determinant of the coefficient matrix of the Eqs. (30), the nontrivial analytical method may be determined from the Eq. (32)

$$\left\{\left([K]+\Delta T[K_T]\right)-\omega_n^2[M]\right\}\begin{Bmatrix}U_n\\W_n\\\phi_n\\\psi_n\end{Bmatrix}=0 \qquad (32)$$

Here $[K]$ and $[K_T]$ are stiffness matrix and coefficient matrix of temperature change, respectively and $[M]$ is the mass matrix. By equaling the obtained determinant from coefficient matrix of above equations, which is a polynomial for ω_n^2, to zero, ω_n is obtained.

4. Results and discussion

In regard to investigate the nanosize effect on the thermos-electro vibration of curved nanobeams, the amounts of nonlocality for the curved porous FGP nanobeams resting on Winkler and Pasternak elastic foundations is considered as constant in the numerical results. To this purpose, the properties materials of curved porous FGP nanobeam made of PZT-4 and PZT-5H, are listed in Table 1. The beam's material composition varies from pure PZT-5H at the bottom surface to pure PZT-4 at the top surface. To validate the results, thermal effect is eliminated and Simply-Simply supported boundary conditions are considered. In addition, material properties are assumed as metal and ceramic for FG curved nanobeams. The non-dimensional fundamental frequencies of the nonlocal FG curved nanobeam without consideration of the piezoelectric properties are compared to the results presented by Hosseini and Rahmani (2016) are listed in Tables 2 and 3 for different power-law index and opening angles. It is observed that the present results agree very well with the given by Ref (Hosseini and Rahmani 2016) and that increasing the nonlocality parameter tends to decrease the natural frequency. The reason is that the presence of the nonlocal effect tends to decrease the stiffness of the nanostructures and hence decrease the values of natural frequencies. The vibration of nano-size curved porous FGP beam resting on elastic foundation and under uniform temperature changes for different values of length scale parameter, nonlocal coefficients, power-law index, porosity parameter and three cases of external electrical voltage are tabloid in Table 4.

The similar conclusions are extracted from this table for the effect of the electric voltage parameter on the dimensionless natural frequencies. It can be noted, from Table 4 that the dimensionless natural frequency decreases while the gradient index increases. From another perspective, this table reveals that the dimensionless natural frequency amplifies with the decrease of the power-law exponent parameter. It can also be observed that the natural frequency increases while length scale parameter (λ) change increasing. In addition, it can be emphasized that the natural Frequency decreases by increasing value of external voltage loading. As it can be deduced from table 4, by increasing porosity parameter, dimensionless natural frequency also increases. Table 5, presents the influences of Winkler (K_W) and Pasternak (K_P) parameters on the dimensionless frequency of curved porous FGP nanobeams with different temperature change values $(\Delta T=0,\ 250,\ 500)$ nonlocality $(\mu^2=0,\ 1,\ 2)$ and porosity parameters $(\vartheta=0,\ 0.2)$ at $(L/h=50,\ \alpha=\pi/2,\ v=+0.01,\ \lambda=2)$. So, various values of Winkler elastic foundation $(K_W=50,\ 100,\ 150)$ and Pasternak elastic foundation $(K_P=10,\ 20,\ 30)$ are considered. It is clear that when the radius of curved FG nanobeam extends to infinity the natural frequencies reach to those of straight nanobeam.

Table 1 constants of material properties (Doroushi *et al*. 2011)

Properties	PZT-4	PZT-5H
$c_{11}\left(Pa\right)$	81.3×10^{9}	60.6×10^{9}
$c_{55}\left(Pa\right)$	25.6×10^{9}	23×10^{9}
$e_{31}\left(C/m^{2}\right)$	-10	-16.604
$e_{15}\left(C/m^{2}\right)$	40.3248	44.9046
$\varepsilon_{11}\left(F/m\right)$	0.6712×10^{-8}	1.5027×10^{-8}
$\varepsilon_{33}\left(F/m\right)$	1.0275×10^{-8}	2.5540×10^{-8}
$\rho\left(Kg/m^{3}\right)$	7500	7500
$\lambda_{1}\left(1/K\right)$	0.2×10^{-5}	1×10^{-5}

Table 2 Comparison of dimensionless natural frequencies of S-S curved FG nanobeams for different amounts of slenderness, mode number and nonlocality where $p=0$ and $\alpha=\pi/3$

L/h	ω_n	$\mu^2=0$		$\mu^2=1$		$\mu^2=2$		$\mu^2=3$		$\mu^2=4$	
		Hosseini and Rahmani 2016	Present	Hosseini and Rahmani 2016	Present	Hosseini and Rahmani 2016	Present	Hosseini and Rahmani 2016	Present	Hosseini and Rahmani 2016	Present
10	$n=1$	8.1991	8.1991	7.8222	7.8222	7.4929	7.4929	7.2020	7.2020	6.9425	6.9425
	$n=2$	35.7451	35.7451	30.2666	30.2666	26.7204	26.7204	24.1855	24.1855	22.2576	22.2576
	$n=3$	77.3993	77.3993	56.3256	56.3256	46.4500	46.4500	40.4308	40.4308	36.2732	36.2732
20	$n=1$	8.2912	8.2912	7.9101	7.9101	7.5771	7.5771	7.2829	7.2829	7.0205	7.0205
	$n=2$	37.2875	37.2875	31.5725	31.5725	27.8733	27.8733	25.2291	25.2291	23.2180	23.2180
	$n=3$	84.3180	84.3180	61.3605	61.3605	50.6022	50.6022	44.0449	44.0449	39.5156	39.5156
50	$n=1$	8.3177	8.3177	7.9353	7.9353	7.6012	7.6012	7.3061	7.3061	7.0429	7.0429
	$n=2$	37.7658	37.7658	31.9776	31.9776	28.2309	28.2309	25.5527	25.5527	23.5159	23.5159
	$n=3$	86.7084	86.7084	63.1000	63.1000	52.0367	52.0367	45.2935	45.2935	40.6359	40.6359

As the value of temperature change increases, the magnitude of dimensionless frequency reduces. As it can be deduced from Table 5, presence of elastic foundation makes the curved porous FGP nanobeam more rigid and increases the vibration frequencies. Moreover, effect of Pasternak medium on curved porous FGP nanobeam is more important than Winkler layer. The value of dimensionless natural frequency reduces as the value of nonlocal parameter increases. This is due to the fact that higher values of nonlocality make the nanobeam softer.

In this section, the effect of voltage on dimensionless natural frequency with investigating different values of length scale parameter and nonlocality can be seen in Fig. 2. Thus, Fig. 2 clearly demonstrates that by increasing external voltage between -0.1 to 0.1, dimensionless natural frequency decreases. However, with the increase the length scale parameter λ between 0 and 3 the natural frequency increases significantly. In addition, Fig. 2 also reveals that the dimensionless natural frequency decreases when the nonlocal parameter becomes greater, disclosing that the effect of the external voltage is more remarkable in the case of curved porous FGP nanobeams. Hence the results show that the nonlocal effect is tending to decrease the stiffness of nanobeams and thus decreases the dimensionless natural frequencies.

The effect of voltage on dimensionless natural frequency with investigating different values of porosity and aspect ratio can be observed in Fig. 3. Thus, Fig. 3 illustrates that with increasing voltage between -0.1 to 0.1, dimensionless natural frequency decreases. In addition, with the increase the porosity parameter ϑ between 0 and 0.3 the natural frequency increases sufficiently. Fig. 3 reveals that the discrepancy between the different values of nonlocality curves decreases when the aspect ratio becomes greater, disclosing that the effect of the aspect ratio is more remarkable in the case of curved porous FGP nanobeams. Hence the results show that the porosity effect is tending to increase the stiffness of nanobeams and thus increase the dimensionless natural frequencies.

Table 3 Comparison of dimensionless natural frequency of S-S curved FG nanobeams for different amounts of slenderness, mode number and nonlocality where $p=1$ and $\alpha=\pi/2$

L/h	ω_n	$\mu^2=0$		$\mu^2=1$		$\mu^2=2$		$\mu^2=3$		$\mu^2=4$	
		Hosseini and Rahmani 2016	Present	Hosseini and Rahmani 2016	Present	Hosseini and Rahmani 2016	Present	Hosseini and Rahmani 2016	Present	Hosseini and Rahmani 2016	Present
10	$n=1$	4.5601	4.5601	4.3504	4.3504	4.1673	4.1673	4.0055	4.0055	3.8612	3.8612
	$n=2$	23.7375	23.7375	20.0993	20.0993	17.7444	17.7444	16.0611	16.0611	14.7808	14.7808
	$n=3$	53.2817	53.2817	38.7745	38.7745	31.9762	31.9762	27.8325	27.8325	24.9704	24.9704
20	$n=1$	4.6675	4.6675	4.4530	4.4530	4.2655	4.2655	4.0999	4.0999	3.9522	3.9522
	$n=2$	25.0039	25.0039	21.1716	21.1716	18.6911	18.6911	16.9179	16.9179	15.5694	15.5694
	$n=3$	58.3285	58.3285	42.4472	42.4472	35.0050	35.0050	30.4689	30.4689	27.3356	27.3356
50	$n=1$	4.7208	4.7208	4.5038	4.5038	4.3142	4.3142	4.1466	4.1466	3.9972	3.9972
	$n=2$	25.5362	25.5362	21.6223	21.6223	19.0889	19.0889	17.2780	17.2780	15.9008	15.9008
	$n=3$	60.4005	60.4005	43.9551	43.9551	36.9551	36.9551	31.5512	31.5512	28.3067	28.3067

Table 4. Variation in the frequency parameter of the curved FGP nanobeams for various amounts of length scale parameter, nonlocality, external electric voltage and power-law exponent $\alpha=\pi/3$, $L/h=10$, $K_W=50$, $K_p=10$, $\Delta T=100$

		$\lambda=0$			$\lambda=2$			$\lambda=4$		
μ^2	$V_0(v)$	Gradient index			Gradient index			Gradient index		
		0	0.5	1	0	0.5	1	0	0.5	1
					$\vartheta=0$					
	-0.05	15.681	15.615	15.588	16.237	16.148	16.116	16.748	16.634	16.595
0	0	15.305	15.153	15.086	15.860	15.683	15.608	16.372	16.168	16.086
	+0.05	14.912	14.665	14.552	15.467	15.193	15.071	15.982	15.680	15.550
	-0.05	15.406	15.350	15.325	15.941	15.865	15.836	16.428	16.330	16.295
1	0	15.032	14.892	14.828	15.564	15.401	15.330	16.051	15.864	15.787
	+0.05	14.641	14.406	14.296	15.171	14.911	14.794	15.659	15.375	15.250
	-0.05	15.164	15.115	15.091	15.681	15.615	15.588	16.149	16.064	16.033
2	0	14.792	14.661	14.599	15.305	15.153	15.086	15.772	15.599	15.526
	+0.05	14.403	14.178	14.072	14.912	14.665	14.552	15.379	15.109	14.989
					$\vartheta=0.2$					
	-0.05	16.807	16.721	16.682	17.379	17.270	17.227	17.899	17.762	17.713
0	0	16.500	16.322	16.239	17.069	16.863	16.774	17.588	17.352	17.255
	+0.05	16.183	15.902	15.771	16.749	16.438	16.298	17.267	16.925	16.776
	-0.05	16.521	16.445	16.407	17.075	16.979	16.939	17.574	17.455	17.410
1	0	16.218	16.050	15.970	16.767	16.576	16.491	17.264	17.047	16.955
	+0.05	15.903	15.636	15.508	16.448	16.154	16.019	16.943	16.621	16.478
	-0.05	16.267	16.197	16.159	16.807	16.721	16.682	17.289	17.184	17.142
2	0	15.967	15.808	15.729	16.500	16.322	16.239	16.980	16.778	16.690
	+0.05	15.655	15.398	15.273	16.183	15.902	15.771	16.660	16.354	16.215

To display the impact of aspect ratio on the dimensionless natural frequency of curved porous FGP resting on elastic foundation for various external voltage $(v=-0.05,\ 0,\ +0.05)$, Fig. 4 presents the frequency results versus aspect ratio with simply-simply boundary

Table 5 Variation in the frequency parameter of the curved FGP nanobeams for various amounts of Winkler and Pasternak parameter, nonlocality, porousity and temperature changes $\alpha = \pi/2$, $L/h = 50$, $V = +0.01$, $\lambda = 2$ $p = 1$

μ^2	Pasternak Parameter	$\Delta T = 0$			$\Delta T = 250$			$\Delta T = 500$		
		Winkler Parameter			Winkler Parameter			Winkler Parameter		
		50	100	150	50	100	150	50	100	150
					$\vartheta = 0$					
0	10	14.664	18.300	21.318	11.831	16.125	19.487	8.0494	13.602	17.463
	20	21.245	23.888	26.260	19.407	22.273	24.805	17.373	20.530	23.256
	30	26.201	28.376	30.391	24.742	27.038	29.149	23.189	25.628	27.849
1	10	14.504	18.171	21.205	11.633	15.979	19.365	7.7557	13.430	17.327
	20	21.131	23.785	26.164	19.284	22.164	24.704	17.237	20.413	23.150
	30	26.105	28.284	30.302	24.642	26.943	29.058	23.083	25.530	27.756
2	10	14.369	18.061	21.110	11.464	15.856	19.262	7.5016	13.284	17.213
	20	21.036	23.697	26.082	19.181	22.072	24.619	17.122	20.314	23.061
	30	26.023	28.205	30.225	24.556	26.862	28.980	22.994	25.446	27.676
					$\vartheta = 0.2$					
0	10	17.442	21.303	24.556	15.664	19.879	23.334	13.655	18.342	22.044
	20	24.476	27.346	29.934	23.251	26.258	28.947	21.956	25.122	27.923
	30	29.870	32.249	34.458	28.880	31.337	33.609	27.854	30.397	32.737
1	10	17.307	21.190	24.455	15.515	19.759	23.230	13.484	18.213	21.934
	20	24.375	27.252	29.845	23.146	26.162	28.856	21.846	25.023	27.831
	30	29.780	32.162	34.372	28.789	31.249	33.523	27.761	30.309	32.650
2	10	17.095	21.013	24.296	15.280	19.571	23.065	13.215	18.011	21.762
	20	24.216	27.103	29.700	22.981	26.009	28.710	21.673	24.866	27.683
	30	29.636	32.020	34.229	28.643	31.107	33.381	27.613	30.165	32.508

conditions at constant value of power-law index (p=1), Winkler & Pasternak elastic foundation $(K_W = 50, K_P = 10)$. As can be seen, at first increment of aspect ratio leads to increasing of dimensionless frequency of curved porous FGP for all of the external voltage. Then, with the increasing of slenderness, it is seen that $v \succ 0, v = 0, v \prec 0$ provided higher, approximately constant and lower dimensional frequency, respectively. In addition, it is observable that higher values of L/h have more significant influence on frequency response. Consequently, the difference between frequency results according to negative and positive values of external electric voltage increases with the rise of aspect ratio. It is pointed that growing of the porosity is cause of increment in the dimensionless frequencies of curved porous FGP. In this section, the effect of the gradient index and external electric voltage on the frequency analysis of nonlocal curved porous FGP nanobeam resting on elastic foundation, is demonstrated in Fig. 5 at constant slenderness ratio *L/h=10*. It can be obviously deduced that; the dimensionless natural frequency reduces with high pace while the power exponent in realm between 0 and 2 than that while power exponent in realm from 2 to 10. In addition, the mentioned results obtained also show that the natural frequencies of the curved porous FGP nanobeam model are evermore lower than those of the classical graded piezoelectric curved beam model. With the increase the external voltage between -0.1 and +0.1, the natural frequency decreases substantially. The results show that by increasing porosity parameter, dimensionless natural frequency also increase.

The fundamental dimensionless frequency as a function of gradient index and temperature changes is presented in Fig. 6 for the curved porous FGP nanobeam. Similarly, it is disclosed that for a simply-simply curved porous FGP nanobeam increasing gradient index and temperature change, leads to reduce the dimensionless natural frequency. Meanwhile as it can be observed from Fig. 5, by increasing porosity parameter, non-dimensional frequency also tends to increase. Fig. 7 illustrates the variation of frequency parameter of curved porous FGP nanobeam respect to mode number for different values of strain gradient parameter at $\alpha = \pi/3$, $p = 1$, $\Delta T = 100$, $\vartheta = 0.1$, $v = 0.1$, $K_W = 50$, $K_P = 10$. For various nonlocality values, a higher mode gives larger natural frequency. It is seen that effect of length scale parameter (λ) on vibration frequency of curved porous FGP nanobeam is more sensitivity at higher modes. For all mode numbers, increasing strain gradient parameter leads to enlargement of frequency parameter. As expected, largest and smallest values of nonlocality have the greatest and smallest frequencies, respectively. In fact, smaller nonlocal parameter make the nanobeam more rigid and lead to larger frequencies.

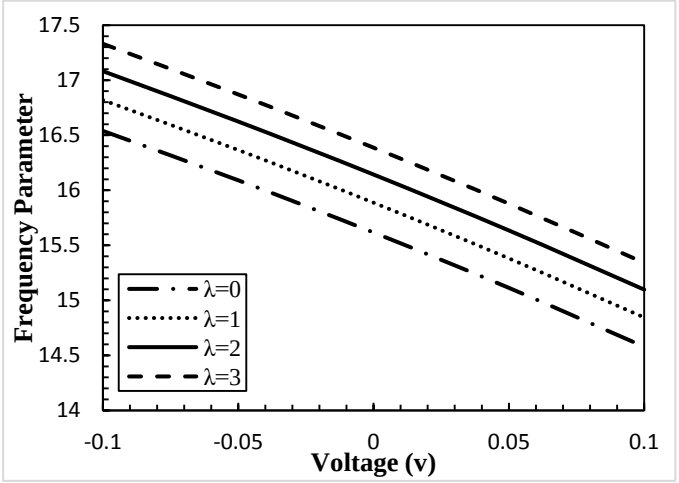

$\mu^2 = 0$

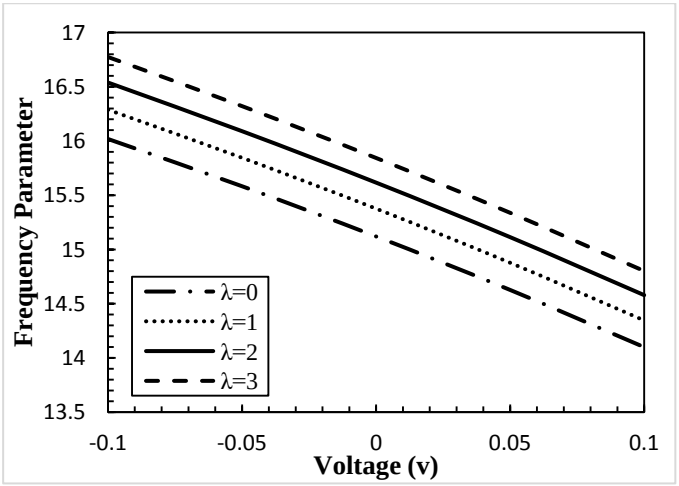

$\mu^2 = 2$

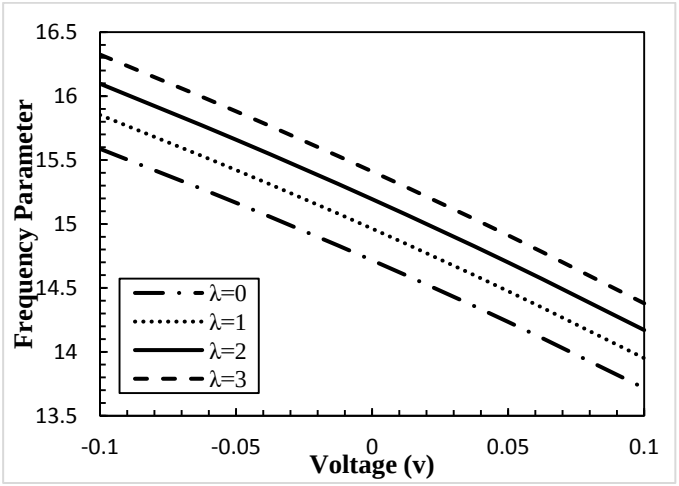

$\mu^2 = 4$

Fig. 2 Variations of the dimensionless natural frequencies of the curved porous FGP nanobeam respect to the voltage with different values of strain gradient parameter and nonlocality $\left(L/h = 10, \alpha = \pi/3, \Delta T = 100, p = 1, \vartheta = 0.1, K_w = 50, K_p = 10\right)$

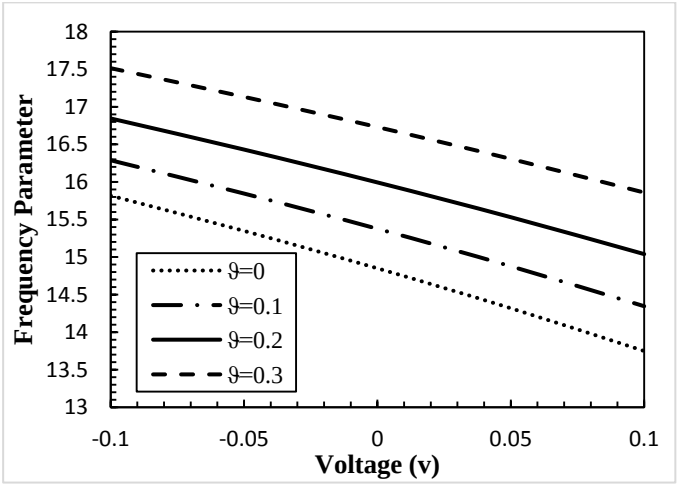

$L/h = 10$

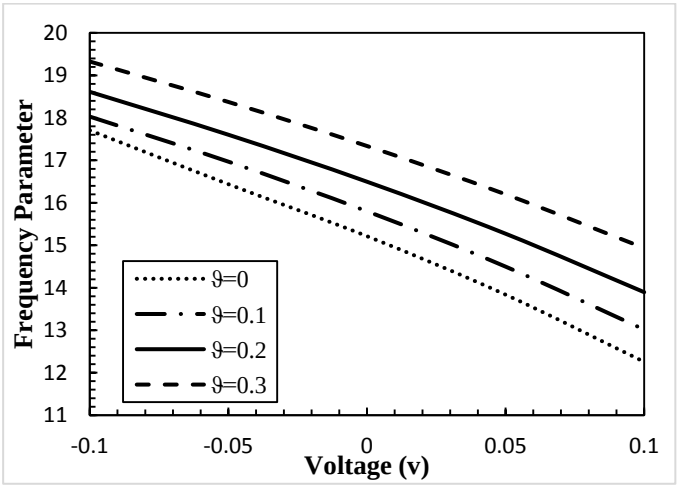

$L/h = 15$

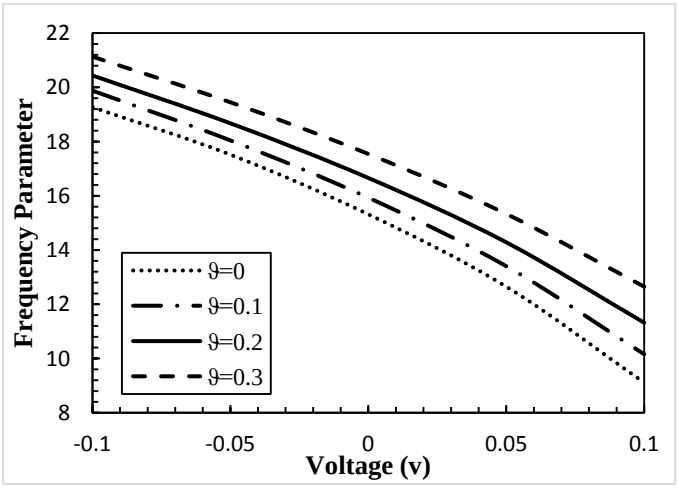

$L/h = 20$

Fig. 3 Variations of the fundamental natural frequencies of the curved porous FGP nanobeam respect to the voltage with different values of porosity parameter and aspect ratio $\left(\alpha = \pi/3, \Delta T = 100, p = 1, \mu^2 = 2, \lambda = 1, K_W = 50, K_p = 10\right)$

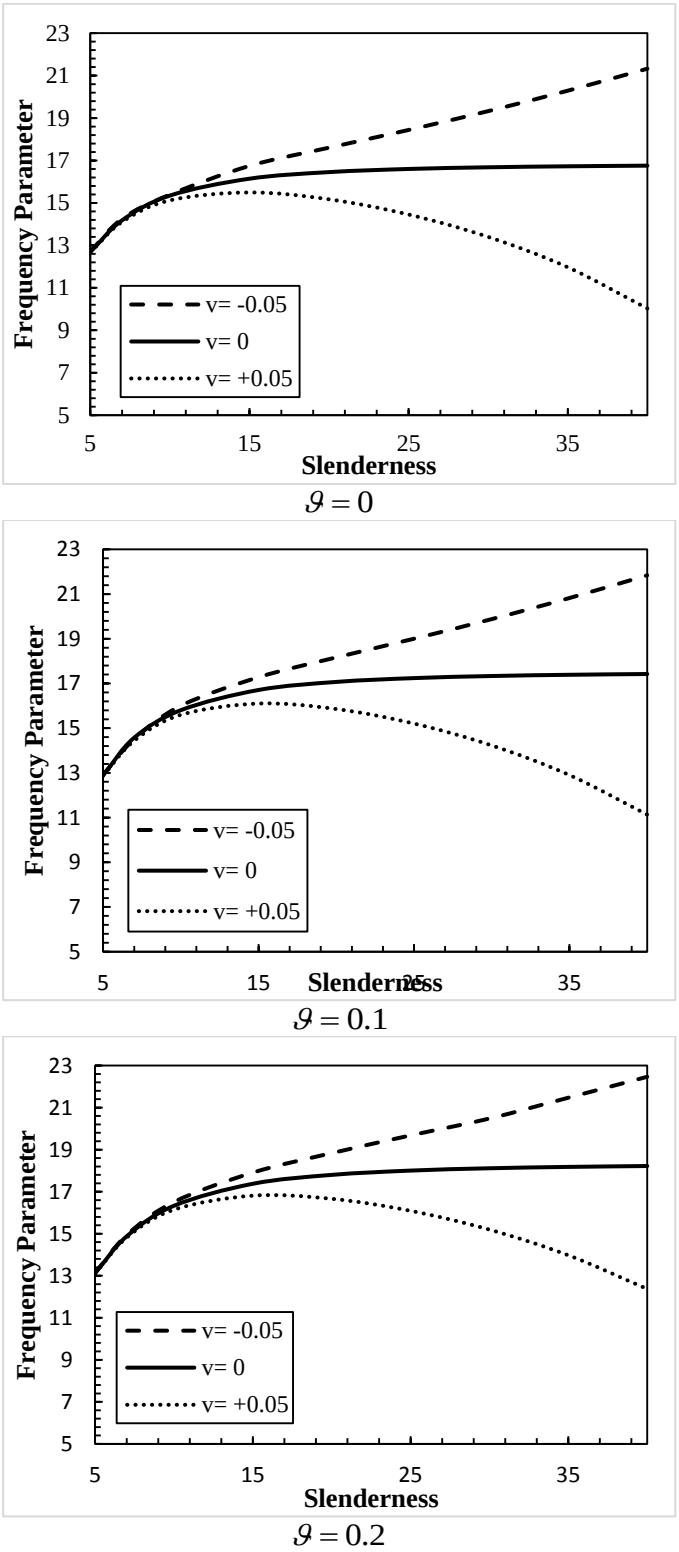

Fig. 4 Influence of aspect ratio on the dimensionless frequency of curved porous FGP resting on elastic foundation for different external voltage and porosity value ($p = 1,\ k_w = 100,\ k_p = 20,\ \mu^2 = 2,\ \lambda = 1,\ \alpha = \pi/4$)

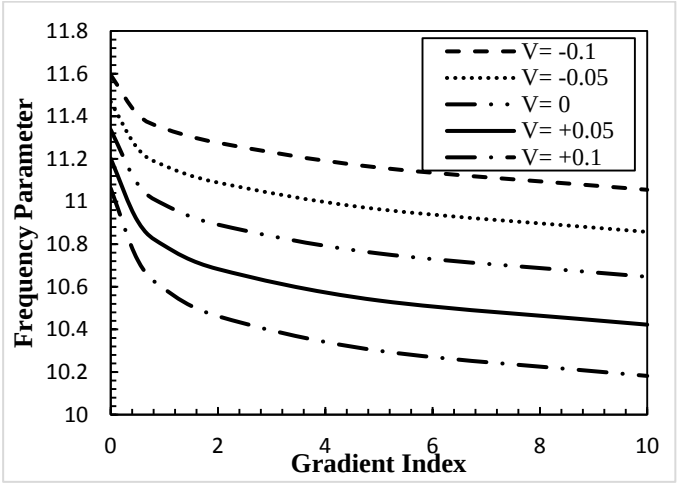

$\vartheta = 0$

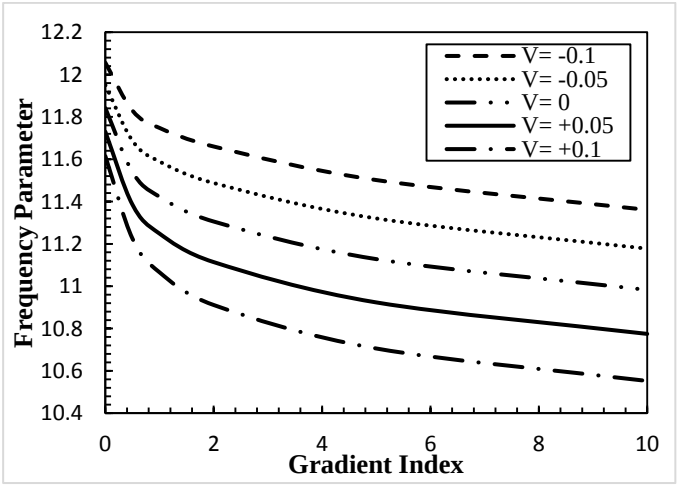

$\vartheta = 0.2$

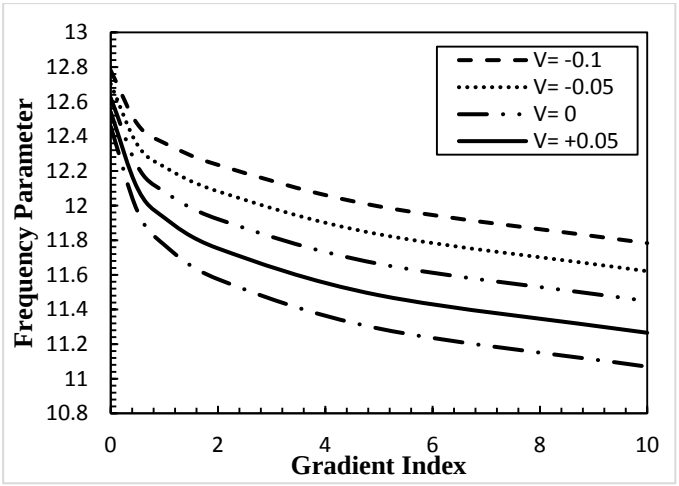

$\vartheta = 0.4$

Fig. 5 Variations of the fundamental natural frequency of the curved porous FGP nanobeam respect gradient index for different amounts of external voltage and porousity $\left(L/h = 10,\ \alpha = \pi/6,\ K_W = 50,\ K_P = 10,\ \lambda = 1,\ \mu^2 = 2,\ \Delta T = 100\right)$.

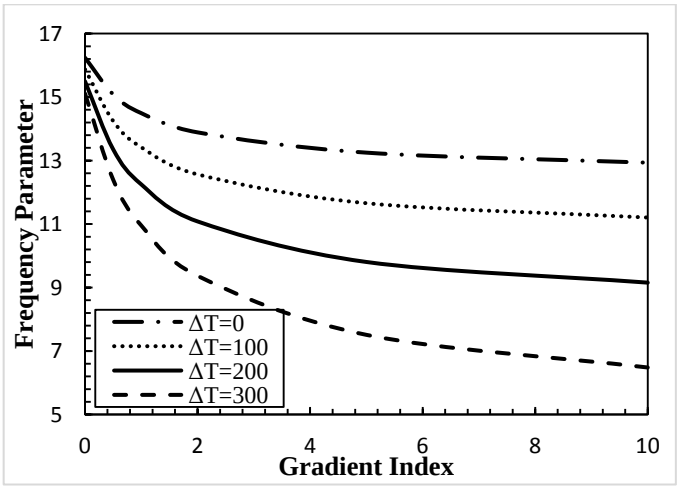

$\vartheta = 0$

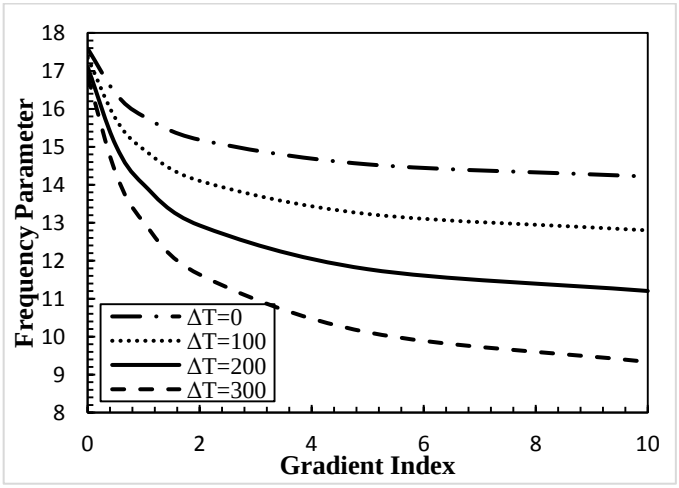

$\vartheta = 0.1$

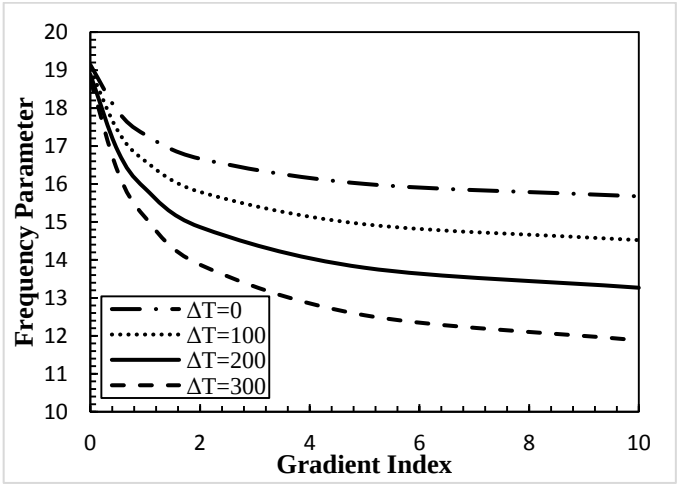

$\vartheta = 0.2$

Fig. 6 Variations of the fundamental natural frequency of the curved porous FGP nanobeam respect gradient index for different amounts of external voltage and porousity $\left(L/h = 50,\ \alpha = \pi/2,\ K_W = 50,\ K_P = 10,\ \lambda = 3,\ \mu^2 = 2,\ \nu = +0.01\right)$

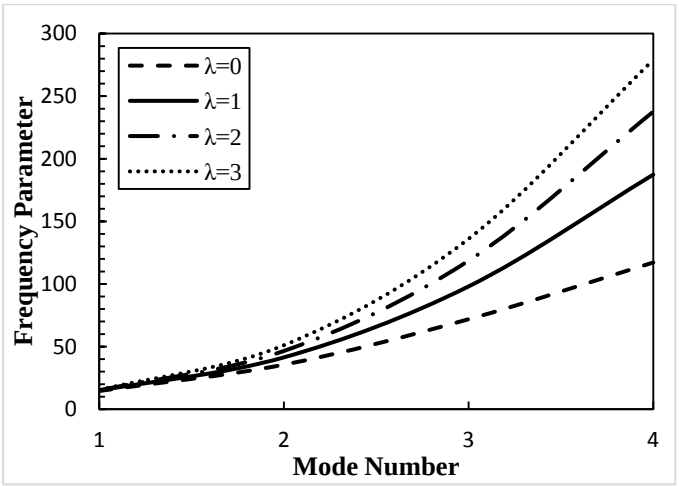

$\mu^2 = 0$

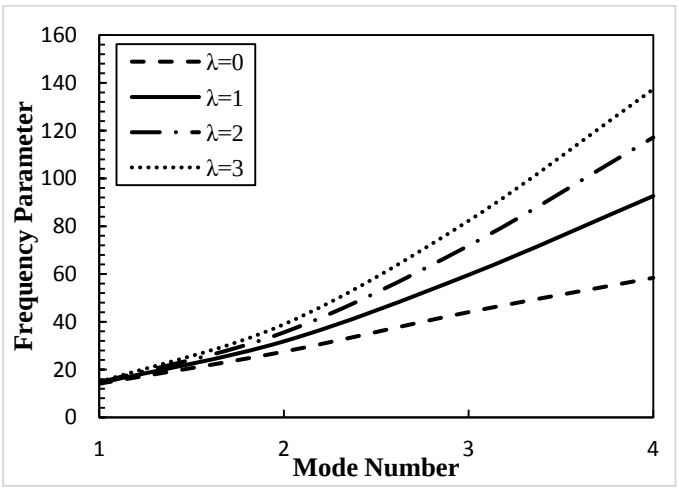

$\mu^2 = 2$

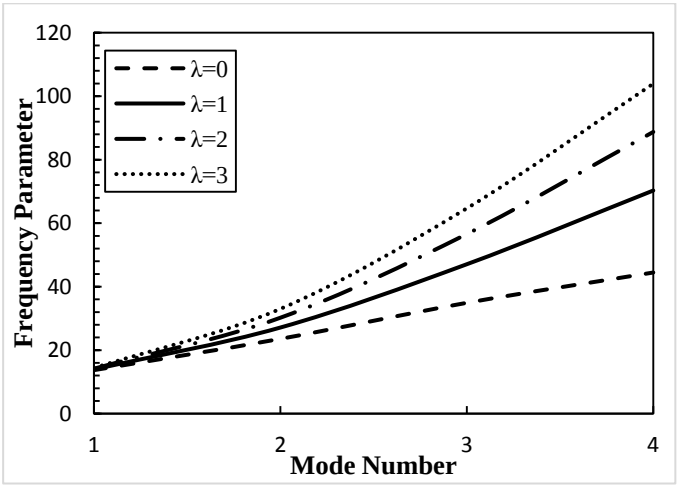

$\mu^2 = 4$

Fig. 7 Effects of strain gradient parameter on dimensionless frequency of curved porous FGP nanobeam with respect to mode number for different nonlocal values $\left(\Delta T = 100,\ \alpha = \pi/3,\ \vartheta = 0.1,\ v = 0.1,\ L/h = 10,\ p = 1,\ K_P = 10,\ K_W = 50\right)$

5. Conclusions

In the proposed investigation, vibration characteristics of embedded porous FG curved piezoelectric nanobeams exposed to thermal loading with different opening angles is implemented within the framework of nonlocal strain gradient elasticity theory in which consider length scale and nonlocality impact. Thermo-Mechanical properties of porous FG curved piezoelectric nanobeams are temperature-dependent and vary in the radial direction based on modified power-law model for approximation of material properties with even distribution of porosities. The governing differential equations of motion and related boundary condition are derived by using Hamilton principle and then solved by applying an analytical exact solution method for Simply-Simply supported boundary condition. Accuracy of the results is examined using available date in the literature. It is indicated that the thermo-mechanical vibration characteristics of embedded curved FG piezo porous nanobeam significantly affected by various parameters such as material graduation index, external electric voltage, Winkler-Pasternak elastic foundation, porosity parameter, temperature environment, length scale parameter, nonlocal parameter, angle of curvature and gradient index. Numerical results show that:

- ✓ By increasing the power-law index value and nonlocal parameter, the non-dimensional frequencies of embedded porous FG curve piezoelectric nanobeams are found to diminish regardless of opening angle and porosity values.
- ✓ Increasing external electric voltage yields reduction of non-dimensional frequency of embedded porous FG piezo curve nanobeam.
- ✓ Effect of slenderness ratio (L/h) on frequencies with respect to external electric voltage is more prominent at its higher values. As slenderness ratio increases, the difference between frequencies results according to negative and positive values of electric voltage increases.
- ✓ Increasing temperature changing yields reduction of natural frequency of embedded porous FG curve piezoelectric nanobeams supposed thermal loading.
- ✓ Increasing strain gradient parameter yields increment of non-dimensional frequency of curved FGM porous nanobeam. However, for the nonlocal parameter this behavior is opposite. Also, impact of strain gradient parameter on frequencies higher mode number is more prominent than lower mode numbers
- ✓ As slenderness ratio increases, the non-dimensional frequencies of embedded porous FG piezoelectric curve nanobeams increase.
- ✓ For the FG piezo curve nanobeams with elastic foundation, increasing the volume fraction of porosity first yields an increase in fundamental frequency for all values of gradient index.

References

Akgoz, B. and Civalek,O. (2011), "Nonlinear vibration analysis of laminated plates resting on nonlinear two-parameters elastic foundations", *Steel Compos. Struct.*, **11**(5), 403-421.

Ansari, R., Gholami, R. and Sahmani, S. (2013), "Size-dependent vibration of functionally graded curved microbeams based on the modified strain gradient elasticity theory", *Archive Appl. Mech*., **83**(10), 1439-1449.

Benveniste, Y. (1995), "Magnetoelectric effect in fibrous composites with piezoelectric and piezomagnetic phases", *Phys. Rev. B.*, **51**(22), 16424.

Bounouara, F., et al., (2016), "A nonlocal zeroth-order shear deformation theory for free vibration of functionally graded nanoscale plates resting on elastic foundation", *Steel Compos. Struct*., **20**(2), 227-249.

Boutahar, L. and Benamar, R. (2016), "A homogenization procedure for geometrically non-linear free vibration analysis of functionally graded annular plates with porosities resting on elastic foundations",. *Ain Shams Engineering Journal*,.

Doroushi, A., Eslami, M. and Komeili, A. (2011), "Vibration analysis and transient response of an FGPM beam under thermo-electro-mechanical loads using higher-order shear deformation theory", *J. Intel. Mat. Syst. Str.*,. **22**(3), 231-243.

Ebrahimi, F. (2013), "Analytical investigation on vibrations and dynamic response of functionally graded plate integrated with piezoelectric layers in thermal environment", *Mech. Adv. Mater. Struct*., **20**(10), 854-870.

Ebrahimi, F. and Barati, M.R. (2016a), "Magneto-electro-elastic buckling analysis of nonlocal curved nanobeams", *European Phys. J. Plus*, **131**(9), 346.

Ebrahimi, F. and Barati, M.R. (2016b), "Static stability analysis of smart magneto-electro-elastic heterogeneous nanoplates embedded in an elastic medium based on a four-variable refined plate theory", *Smart Mater. Struct*., **25**(10), 105014.

Ebrahimi, F. and Barati, M.R. (2016c), "Temperature distribution effects on buckling behavior of smart heterogeneous nanosize plates based on nonlocal four-variable refined plate theory", *Int. J. Smart Nano Mater*., 1-25.

Ebrahimi, F. and Barati, M.R. (2016d), "An exact solution for buckling analysis of embedded piezoelectro-magnetically actuated nanoscale beams", *Adv. Nano Res*., **4**(2), 65-84.

Ebrahimi, F. and Barati, M.R. (2016e), "Buckling analysis of smart size-dependent higher order magneto-electro-thermo-elastic functionally graded nanosize beams", *J. Mech*., 1-11.

Ebrahimi, F. and Barati, M.R. (2016f), "A nonlocal higher-order shear deformation beam theory for vibration analysis of size-dependent functionally graded nanobeams", *Arabian J. Sci. Eng*., **41**(5), 1679-1690.

Ebrahimi, F. and Barati, M.R. (2016g), "Vibration analysis of smart piezoelectrically actuated nanobeams subjected to magneto-electrical field in thermal environment", *J. Vib. Control*, 1077546316646239.

Ebrahimi, F. and Barati, M.R. (2016h), "Buckling analysis of nonlocal third-order shear deformable functionally graded piezoelectric nanobeams embedded in elastic medium", *J. Brazilian Soc. Mech. Sci. Eng*., 1-16.

Ebrahimi, F. and Barati, M.R. (2016i), "Small scale effects on hygro-thermo-mechanical vibration of temperature dependent nonhomogeneous nanoscale beams", *Mech. Adv. Mater. Struct*. , (just-accepted).

Ebrahimi, F. and Barati, M.R. (2016j), "Dynamic modeling of a thermo–piezo-electrically actuated nanosize beam subjected to a magnetic field", *Appl. Phys, A*, **122**(4), 1-18.

Ebrahimi, F. and Barati, M.R. (2016k), "Magnetic field effects on buckling behavior of smart size-dependent graded nanoscale beams", *European Phys. J. Plus*, **131**(7), 1-14.

Ebrahimi, F. and Barati, M.R. (2016l), "Vibration analysis of nonlocal beams made of functionally graded material in thermal environment", *European Phys. J. Plus*, **131**(8), 279.

Ebrahimi, F. and Barati, M.R. (2017a), "Hygrothermal effects on

vibration characteristics of viscoelastic FG nanobeams based on nonlocal strain gradient theory", *Compos. Struct*., **159**, 433-444.

Ebrahimi, F. and Barati, M.R. (2017b), "A nonlocal strain gradient refined beam model for buckling analysis of size-dependent shear-deformable curved FG nanobeams", *Compos. Struct*., **159**, 174-182.

Ebrahimi, F. and Daman, M. (2016a), "An investigation of radial vibration modes of embedded double-curved-nanobeam-systems", *Cankaya Univ J Sci Eng*,. **13**, 058-079.

Ebrahimi, F. and Daman, M. (2016b), "Dynamic modeling of embedded curved nanobeams incorporating surface effects", *Coupled Syst. Mech.*,. **5**(3), 255-267.

Ebrahimi, F. and Daman, M. (2016c), "Investigating surface effects on thermomechanical behavior of embedded circular curved nanosize beams", *J. Engineering*, **2016**.

Ebrahimi, F. and Daman, M. (2017), "Analytical investigation of the surface effects on nonlocal vibration behavior of nanosize curved beams", *Adv. Nano Res*,. **5**(1), 35-47.

Ebrahimi, F. and Hosseini, S.H.S. (2016a), "Double nanoplate-based NEMS under hydrostatic and electrostatic actuations", *European Phys. J. Plus*, **131**(5), 1-19.

Ebrahimi, F. and Hosseini, S.H.S. (2016b), "Nonlinear electroelastic vibration analysis of NEMS consisting of double-viscoelastic nanoplates", *Appl. Phys. A*, **122**(10), 922.

Ebrahimi, F. and Hosseini, S.H.S. (2016c), "Thermal effects on nonlinear vibration behavior of viscoelastic nanosize plates", *J. Therm. Stresses*, **39**(5), 606-625.

Ebrahimi, F. and Jafari, A. (2016a), "Thermo-mechanicalvibration analysis of temperature-dependent porous FG beams based on Timoshenko beam theory", *Struct. Eng. Mech*., **59**(2), 343-371.

Ebrahimi, F. and Jafari, A. (2016b), "A higher-order thermomechanical vibration analysis of temperature-dependent FGM beams with porosities", *J. Engineering*.

Ebrahimi, F. and Jafari, A. (2016c), "Buckling behavior of smart MEE-FG porous plate with various boundary conditions based on refined theory", *Adv. Mater. Res*., **5**(4), 279-298.

Ebrahimi, F. and Jafari, A. (2017), "A four-variable refined shear-deformation beam theory for thermo-mechanical vibration analysis of temperature-dependent FGM beams with porosities", *Mech. Adv. Mater. Struct*., 1-13.

Ebrahimi, F. and Mokhtari, M. (2015), "Transverse vibration analysis of rotating porous beam with functionally graded microstructure using the differential transform method", *J. Brazilian Soc. Mech. Sci. Eng*., **37**(4), 1435-1444.

Ebrahimi, F. and Nasirzadeh, P. (2015), "A nonlocal Timoshenko beam theory for vibration analysis of thick nanobeams using differential transform method",. *J. Theor. Appl. Mech*., **53**(4), 1041-1052.

Ebrahimi, F. and Salari, E. (2015), "Thermo-mechanical vibration analysis of nonlocal temperature-dependent FG nanobeams with various boundary conditions", *Compos B*, **78**, 272-290.

Ebrahimi, F. and Salari, E. (2015a), "Size-dependent thermo-electrical buckling analysis of functionally graded piezoelectric nanobeams", *Smart Mater. Struct*., **24**(12), 125007, 2015

Ebrahimi, F. and Salari, E. (2015b), "Nonlocal thermo-mechanical vibration analysis of functionally graded nanobeams in thermal environment", *Acta Astronautica*, **113**, 29-50.

Ebrahimi, F. and Salari, E. (2015c), "Size-dependent free flexural vibrational behavior of functionally graded nanobeams using semi-analytical differential transform method", *Composites Part B: Eng.*,. **79**, 156-169.

Ebrahimi, F. and Salari, E. (2015d), "A semi-analytical method for vibrational and buckling analysis of functionally graded nanobeams considering the physical neutral axis position", *CMES: Comput. Model. Eng. Sci.*, **105**, 151-181.

Ebrahimi, F. and Salari, E. (2015e), "Thermal buckling and free vibration analysis of size dependent Timoshenko FG nanobeams in thermal environments", *Compos. Struct*., **128**, 363-380.

Ebrahimi, F. and Salari, E. (2015f), "Thermo-mechanical vibration analysis of nonlocal temperature-dependent FG nanobeams with various boundary conditions", *Compos. B*, **78**, 272-290.

Ebrahimi, F. and Salari, E. (2016), "Effect of various thermal loadings on buckling and vibrational characteristics of nonlocal temperature-dependent functionally graded nanobeams", *Mech. Adv. Mater. Struct*., **23**(12), 1379-1397.

Ebrahimi, F. and Zia, M. (2015), "Large amplitude nonlinear vibration analysis of functionally graded Timoshenko beams with porosities", *Acta Astronautica*, **116**, 117-125.

Ebrahimi, F., Barati, M.R. and Haghi, P. (2017), "Thermal effects on wave propagation characteristics of rotating strain gradient temperature-dependent functionally graded nanoscale beams", *J. Therm. Stresses*, **40**(5), 535-547.

Ebrahimi, F., Ehyaei, J. and Babaei, R. (2016), "Thermal buckling of FGM nanoplates subjected to linear and nonlinear varying loads on Pasternak foundation", *Adv. Mater. Res*., **5**(4), 245-261.

Ebrahimi, F., Ghadiri, M., Salari, E., Hoseini, S.A.H. and Shaghaghi, G.R. (2015b), "Application of the differential transformation method for nonlocal vibration analysis of functionally graded nanobeams", *J. Mech. Sci. Tech*., **29**, 1207-1215.

Ebrahimi, F., Ghasemi, F. and Salari, E. (2016a), "Investigating thermal effects on vibration behavior of temperature-dependent compositionally graded Euler beams with porosities", *Meccanica*, **51**(1), 223-249.

Ebrahimi, F., Jafari, A. and Barati, M.R. (2016), "Free vibration analysis of smart porous plates subjected to various physical fields considering neutral surface position", *Arabian J. Sci. Eng.*, **5**(42), 1865-1881.

Ebrahimi, F., Jafari, A. and Barati, M.R. (2017), "Vibration analysis of magneto-electro-elastic heterogeneous porous material plates resting on elastic foundations", *Thin. Wall. Struct*., **119**, 33-46.

Ebrahimi, F., Salari, E. and Hosseini, S.A.H. (2015), "Thermomechanical vibration behavior of FG nanobeams subjected to linear and non-linear temperature distributions", *J. Therm. Stresses*, **38**(12), 1360-1386.

Ebrahimi, F., Salari, E. and Hosseini, S.A.H. (2016c), "In-plane thermal loading effects on vibrational characteristics of functionally graded nanobeams", *Meccanica*, **51**(4), 951-977.

Eltaher, M., Emam, S.A. and Mahmoud, F. (2012), "Free vibration analysis of functionally graded size-dependent nanobeams", *Appl. Math. Comput.*,. **218**(14), 7406-7420.

Eringen, A.C. (1972a), "Nonlocal polar elastic continua", *Int. J. Eng. Sci*., **10**(1), 1-16.

Eringen, A.C. (1972b), "Linear theory of nonlocal elasticity and dispersion of plane waves", *Int. J. Eng. Sci.*, **10**(5), 425-435.

Eringen, A.C. (1983), "On differential equations of nonlocal elasticity and solutions of screw dislocation and surface waves", *J. Appl. Phys.*, **54**(9), 4703-4710.

Eringen, A.C. (2002), *Nonlocal continuum field theories*,: Springer Science & Business Media.

Fallah, A. and Aghdam, M.M. (2011), "Nonlinear free vibration and post-buckling analysis of functionally graded beams on nonlinear elastic foundation", *European J. Mech. –A /Solids*, **30**(4), 571-583.

Fleck, N.A. and Hutchinson, J.W. (1993), "A phenomenological theory for strain gradient effects in plasticity", *J. Mech. Phys. Solids*,. **41**(12), 1825-1857.

Harshe, G., Dougherty, J. and Newnham, R. (1993), "Theoretical modelling of multilayer magnetoelectric composites", *Int. J. Appl. Electromagnetics Mater.*. **4**(2), 145-145.

Hashemi, S.H., Taher, H.R.D. and Omidi, M. (2008), "3-D free vibration analysis of annular plates on Pasternak elastic

foundation via p-Ritz method", *J. Sound Vib.*, **311**(3), 1114-1140.
Hosseini, S. and Rahmani, O. (2016), "Free vibration of shallow and deep curved FG nanobeam via nonlocal Timoshenko curved beam model", *Appl. Phys. A*,. **122**(3), 1-11.
Huang, Z., Lü, C. and Chen, W. (2008), "Benchmark solutions for functionally graded thick plates resting on Winkler–Pasternak elastic foundations", *Compos. Struct*., **85**(2), 95-104.
Kananipour, H., Ahmadi, M. and Chavoshi, H. (2014), "Application of nonlocal elasticity and DQM to dynamic analysis of curved nanobeams", *Latin Am. J. Solids Struct.*,. **11**(5), 848-853.
Koizumi, M. and Niino, M. (1995), "Overview of FGM Research in Japan", *Mrs Bulletin*, **20**(1), 19-21.
Komijani, M., Reddy, J. and Eslami, M. (2014), "Nonlinear analysis of microstructure-dependent functionally graded piezoelectric material actuators", *J. Mech. Phys. Solids*,. **63**, 214-227.
Lam, D.C.C., *et al.* (2003), "Experiments and theory in strain gradient elasticity", *J. Mech. Phys. Solids*,. **51**(8), 1477-1508.
Li, L. and Hu, Y. (2015), "Buckling analysis of size-dependent nonlinear beams based on a nonlocal strain gradient theory", *Int. J. Eng. Sci.*,. **97**, 84-94.
Li, L., Hu, Y. and Ling, L. (2015), "Flexural wave propagation in small-scaled functionally graded beams via a nonlocal strain gradient theory", *Compos. Struct*., **133**, 1079-1092.
Li, L., Li, X. and Hu, Y. (2016), "Free vibration analysis of nonlocal strain gradient beams made of functionally graded material", *Int. J. Eng. Sci*., **102**, 77-92.
Lim, C., Zhang, G. and Reddy, J. (2015), "A higher-order nonlocal elasticity and strain gradient theory and its applications in wave propagation", *J. Mech. Phys. Solids*,. **78**, 298-313.
Malekzadeh, P. (2009), "Three-dimensional free vibration analysis of thick functionally graded plates on elastic foundations", *Compos. Struct.*, **89**(3), 367-373.
Malekzadeh, P., Haghighi, M.G. and Atashi, M. (2010), "Out-of-plane free vibration of functionally graded circular curved beams in thermal environment", *Compos. Struct*., **92**(2), 541-552.
Mechab, I., et al., (2016), "Free vibration analysis of FGM nanoplate with porosities resting on Winkler Pasternak elastic foundations based on two-variable refined plate theories", *J. Brazilian Soc. Mech. Sci. Eng*., 1-19.
Mortensen, A. and Suresh, S. (2013), "Functionally graded metals and metal-ceramic composites: Part 1 Processing", *International Materials Reviews*.
Nan, C.W. (1994), "Magnetoelectric effect in composites of piezoelectric and piezomagnetic phases", *Phys. Rev. B*,. **50**(9), 6082.
Pradhan, S. and Murmu, T. (2009), "Thermo-mechanical vibration of FGM sandwich beam under variable elastic foundations using differential quadrature method", *J. Sound Vib.*, **321**(1), 342-362.
Wang, C.M. and Duan, W.H. (2008), "Free vibration of nanorings/arches based on nonlocal elasticity", *J. Appl. Phys.*, **104**(1), 014303.
Wattanasakulpong, N., Prusty, B.G. and Kelly, D.W. (2011), "Thermal buckling and elastic vibration of third-order shear deformable functionally graded beams", *Int. J. Mech. Sci.*, **53**(9), 734-743.
Yahia, S.A., *et al.* (2015), "Wave propagation in functionally graded plates with porosities using various higher-order shear deformation plate theories", *Struct. Eng. Mech.*, **53**(6), 1143-1165.
Yan, Z. and Jiang, L. (2011), "Electromechanical response of a curved piezoelectric nanobeam with the consideration of surface effects", *J. Phys. D: Appl. Phys.*,. **44**(36), 365301.
Ying, J., Lü, C. and Chen, W. (2008), "Two-dimensional elasticity solutions for functionally graded beams resting on elastic foundations", *Compos. Struct.*, **84**(3), 209-219.
Zhou, D., *et al.* (2006), "Three-dimensional free vibration of thick circular plates on Pasternak foundation", *J. Sound Vib*., **292**(3), 726-741.

FC